THE ASTROPHYSICAL JOURNAL, 471:949–957, 1996 November 10

V1315 AQUILAE AND THE NATURE OF SW SEXTANTIS STARS

COEL HELLIER
Department of Physics, Keele University, Keele, Staffordshire, ST5 5BG, England UK;
ch@astro.keele.ac.uk
Received 1996 April 8; accepted 1996 May 13

ABSTRACT

Optical spectroscopy of the nova-like variable V1315 Aql shows strong single-peaked emission lines, high-velocity s-waves in the wings of the lines, and two distinct absorption components. In order to explain all the features, I suggest that disk overflow accretion has to be combined with an accretion disk wind. The absorption is probably caused by the accretion stream as it flows over the disk and by P Cygni troughs produced by the wind. If correct, this model can account for the peculiarities of the emission lines in SW Sex stars. Both disk overflow and the strong wind might result from a high mass transfer rate.

Subject headings: accretion, accretion disks — binaries: close — novae, cataclysmic variables — stars: individual: (V1315 Aquilae)

1. INTRODUCTION

Nova-like variables are thought to be cataclysmic binaries with high mass transfer rates, such that they do not show the accretion disk instabilities associated with dwarf novae. Thorstensen et al. (1991) drew attention to a group of nova-like variables showing peculiar behavior, including emission-line profiles grossly distorted from those expected from an axisymmetric disk, and absorption in the core of the line occurring at orbital phase 0.5 (when the red dwarf secondary is farthest from us). The emission lines are also single peaked, whereas accretion disks produce double peaks. These stars, dubbed "SW Sex stars" by Thorstensen et al. (1991), tend to have orbital periods of 3–4 hr and be eclipsing. It is unclear whether such systems are truly different (for instance, the tendency to be eclipsing is almost certainly a selection effect, in that the other symptoms are seen more easily in highly inclined binaries); however, the term "SW Sex star" is at least a useful shorthand to denote these characteristics.

Shafter, Hessman, & Zhang (1988) suggested that the distorted emission-line profiles were caused by the accretion stream from the secondary star penetrating into the accretion disk. Then Hellier et al. (1989) found strong evidence that the stream in EX Hya during outburst was overflowing the initial impact with the disk and continuing on a ballistic trajectory to a second impact much nearer the white dwarf. At the same time, Lubow (1989) advocated this idea on theoretical grounds.

In our previous paper on SW Sex stars (Hellier & Robinson 1994, hereafter HR94) we investigated the disk overflow model by computing the expected emission-line profiles and comparing them to spectroscopy of PX And. We found that emission from the reimpact point of the stream on the disk, near to the location calculated by Lubow (1989), explained the asymmetric emission profiles. Further, we proposed that the stream was seen in absorption between the initial impact with the disk and its later reimpact, explaining the peculiar phase 0.5 absorption features and providing a good match to their velocity variations. We proposed that substantial disk overflow was the property distinguishing SW Sex stars from other cataclysmic variables (CVs).

That paper still left work to be done. The time resolution of the data was insufficient to test whether the eclipse behavior of the lines was consistent with the model, and further, the disk overflow model alone did not provide a convincing explanation for the single-peaked line profiles, particularly of He II λ4686, seen in SW Sex stars (e.g., Dhillon, Marsh, & Jones 1991). In this paper, I present new spectroscopy of the SW Sex star V1315 Aql, covering the He II λ4686 line as well as Balmer lines. In order to explain all the lines, the disk overflow idea has to be combined with a mechanism producing single peaks, such as a strong accretion disk wind. I create, for the first time, simple reproductions of lines containing both components, and I show that these are phenomenologically similar to the spectra of SW Sex stars. For details of other models for SW Sex stars, see Thorstensen et al. (1991) and Dhillon et al. (1991).

2. THE EPHEMERIS

To secure the phasing of the spectroscopy, I observed an eclipse photometrically on the night of 1994 August 15 using the McDonald Observatory 0.9 m telescope and CCD camera. This gave a mideclipse timing of HJD 2,449,579.6195(3). Combining this with timings published by Dhillon et al. (1991) and Annis (1986) gives the following ephemeris, which is only marginally different from that published by Dhillon et al.:

$$\mathrm{HJD}_{\mathrm{ecl}} = 2{,}445{,}902.70088(12) + 0.139689938(9)E \ .$$

3. OBSERVATIONS

With assistance from Cyndi Froning, I observed V1315 Aql with the McDonald Observatory 2.1 m telescope on the nights of 1994 July 2, 3, 4, and 7. The ES2 spectrograph and TI1 CCD covered the range Hγ to Hβ with a resolution of 1.8 Å. We obtained 224 spectra, each with a 5 minute integration time, covering more than seven orbital cycles. The average of the spectra is shown in Figure 1, where strong Balmer and helium emission lines are obvious. I then allocated the spectra into 30 phase bins around the orbital cycle, using the above ephemeris. The phase binned Hβ and He II λ4686 lines are shown in Figures 2 and 3.

4. INTERPRETATION

The phase-resolved line profiles are complex, with several components interacting. In what follows, I present my interpretation of the data, based on the disk overflow model.

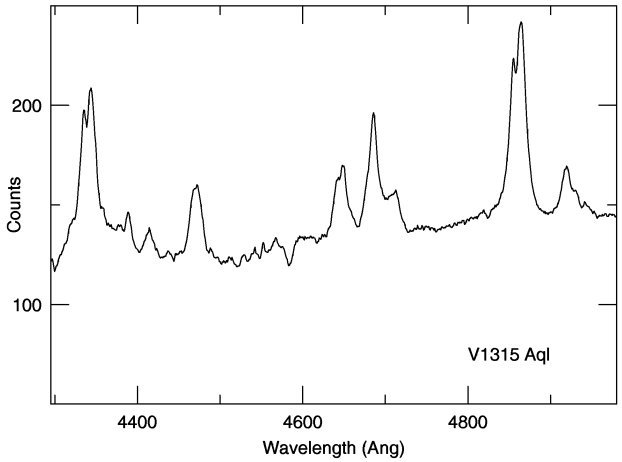

FIG. 1.—The average of the 224 V1315 Aql spectra, showing strong Balmer, He I, He II, and Bowen blend emission. The feature at 4580 Å is a chip defect.

Much of the interpretation is not unique, so it has to be judged by how well the simulations reproduce the data. It is easiest to discuss the interpretation with reference to the schematic diagrams of Figures 4 and 5, comparing them to the gray-scale profiles in Figure 6. I start with He II λ4686, since this is the simplest line, and then I turn to Hβ. The other lines, as far as their lower signal-to-noise ratio (S/N) enables one to judge, behave similarly to either Hβ (Hγ, He I λ4471) or to He II λ4686 (the other He II lines and the Bowen blend).

4.1. He II λ4686

The He II λ4686 line consists largely of a single-peaked profile, varying in velocity with maximum redshift near phase 0.75. This is unlikely to be disk emission, which would be double-peaked, and it cannot be emission from the stream reimpact site of the disk overflow model, since this would have a later phasing and a higher velocity amplitude. Instead, I concur with previous suggestions (e.g., Honeycutt, Schlegel, & Kaitchuck 1986; Dhillon et al. 1991) that such profiles are probably due to an accretion disk wind driven from the inner disk or boundary layer.

This is supported by the modeling of Hoare (1994). He finds that a bipolar wind from a high-inclination binary gives a single-peaked line profile, roughly symmetric about the rest wavelength, similar to that in my data. Since this line is relatively optically thin, there is little blueshifted absorption associated with the emission. The width of He II λ4686 is hard to estimate due to contamination from the Bowen blend and He I λ4713, but it probably extends between 4665 and 4706 Å, corresponding to a full width of 2600 km s^{-1}. This is comparable with Hoare's model line, which has fallen to $\sim$7% of its peak intensity by that velocity.

The He II λ4686 line is eclipsed to a similar degree as the continuum (Figs. 2, 3, and 6 are normalized to the continuum; thus, a similar intensity implies a variation following the continuum—the eclipse is seen, though, as a decrease in S/N). This concurs with Hoare's models, in which the line-forming region at $\sim 4\,R_{WD}$ shows a deep eclipse. We cannot, however, make a detailed comparison with the current data

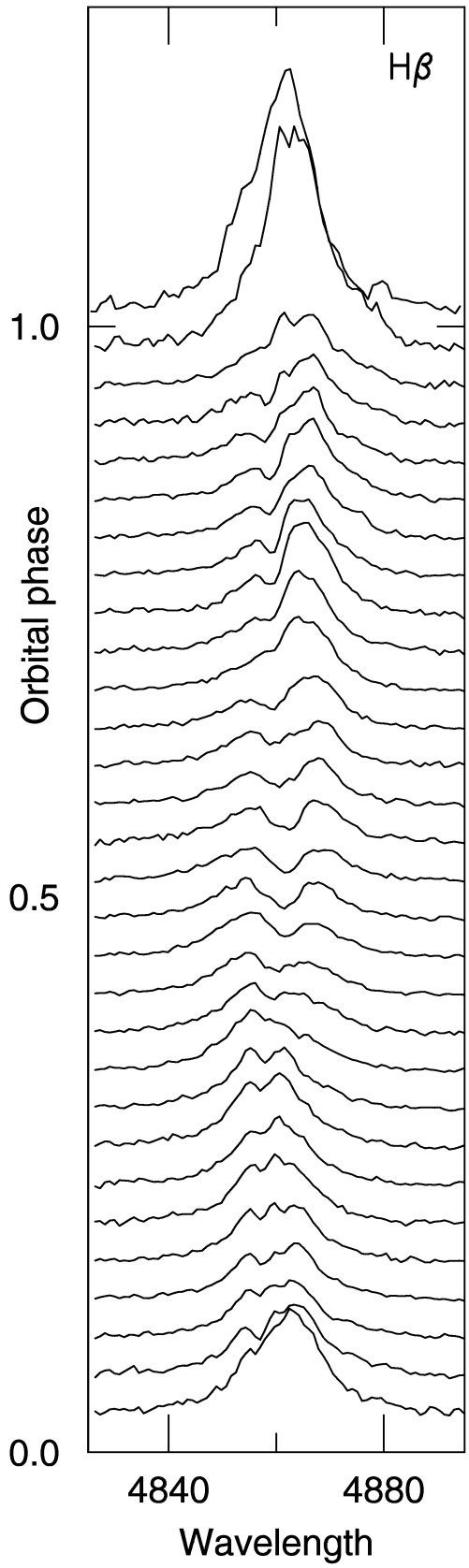

FIG. 2.—Orbitally phase-binned Hβ profiles normalized to the continuum.

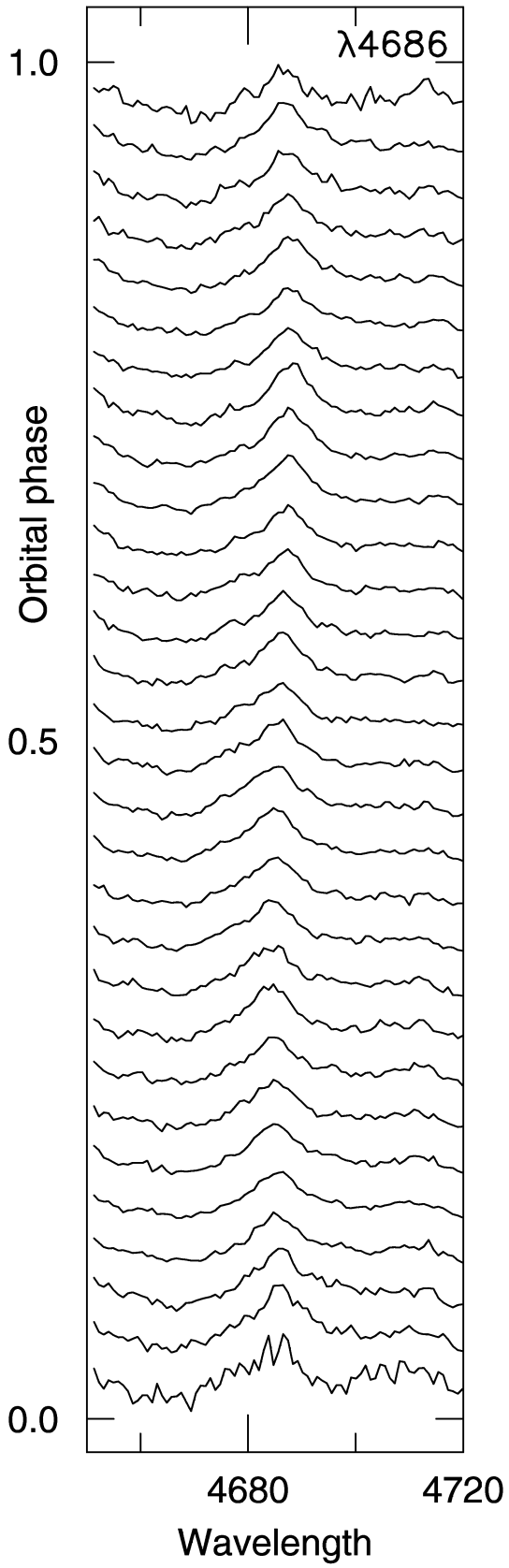

FIG. 3.—Orbitally phase-binned He II λ4686 profiles normalized to the continuum.

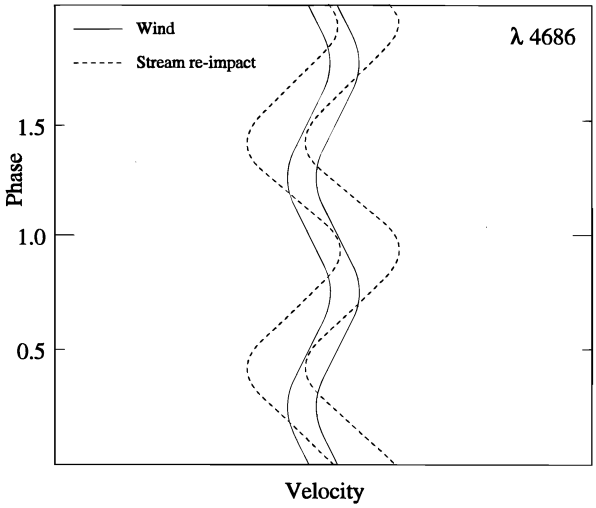

FIG. 4.—Schematic interpretation of the He II λ4686 profiles, composed of wind emission and emission from the stream reimpact site.

due to its poor time resolution (0.03 in phase) and low S/N during eclipse.

There is a further component in the He II λ4686 profile, much weaker than the wind component. This has a higher velocity and a maximum redshift at phase ~0.9. In Figure 6 it is seen most readily at its bluest extreme at phase 0.4. (The emission even farther to the blue at -2000 km s^{-1} is the edge of the Bowen blend; similarly, He I λ4713 lies to the red, so the intensity never declines to true continuum in this figure.) Further support for the existence of this component is provided by its clear presence in the Hβ line (see § 4.2) and in the distortion of the radial velocity motion from that of the white dwarf (see § 6). I suggest that the broad component arises where the overflowing stream reimpacts the disk.

To simulate the line profile produced by the combination of reimpact emission and a wind, I have used the simulation program described in HR94. This computes the velocity of material in free-fall, following the trajectory of the stream flowing over the accretion disk until it reimpacts, as computed by Lubow (1989). The program then calculates the

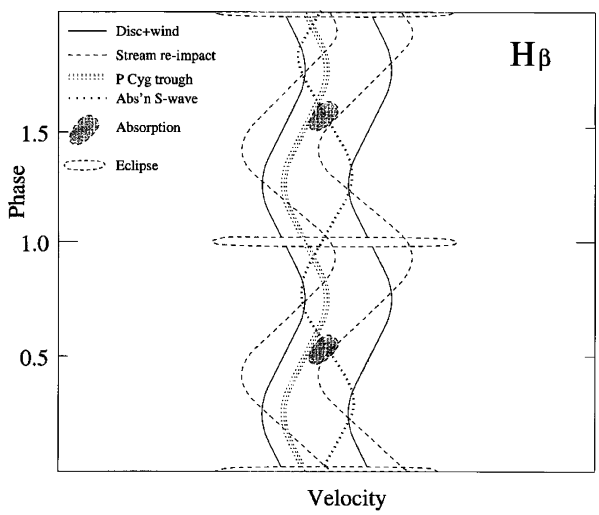

FIG. 5.—Schematic interpretation of the Hβ profiles. We see emission from a wind, the disk, and the reimpact site, together with P Cygni absorption and stream absorption. The line is relatively much brighter in eclipse.

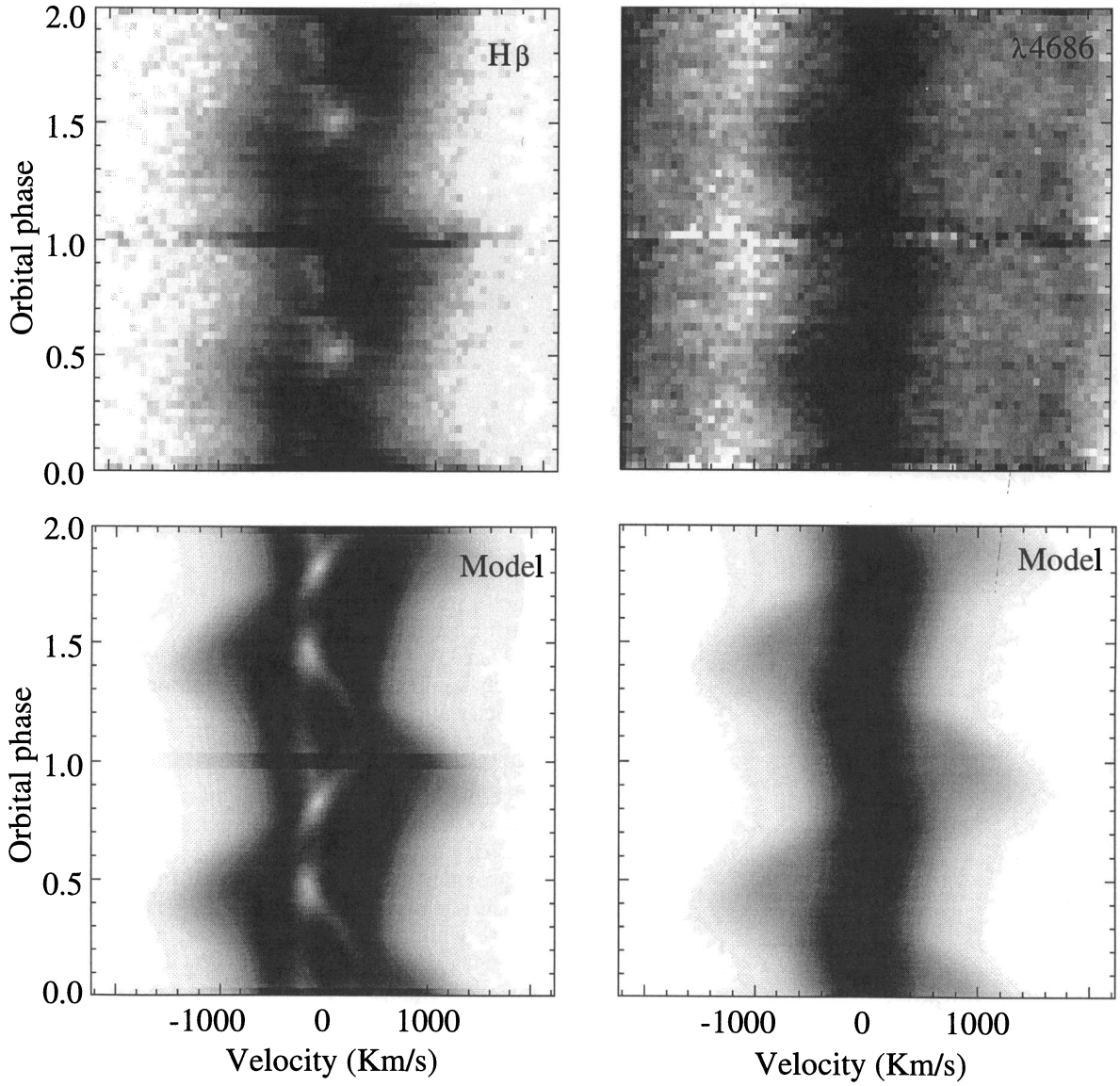

FIG. 6.—The orbitally phase-binned Hβ and He II λ4686 profiles (*top*) together with model simulations. The decomposition into components is illustrated schematically in Figs. 4 and 5. The model, described in the text, combines the components and attempts to match the observed profiles. Although the model velocities are calculated correctly, the relative intensities of the model components are arbitrary.

projection of the velocities around the orbit, to produce synthetic line profiles. As was done in HR94, I took the velocity of the emission to be the mean of the velocities of the stream and local disk, supposing that there is a strong interaction between them. For the emission profile, I used a Gaussian with a width (σ) of 25% of that velocity. To this, I added a synthetic wind profile, taking the bipolar profile from Figure 5 of Hoare (1994) and moving it with the orbital motion of the white dwarf. For modeling purposes, I used primary and secondary masses of 0.70 and 0.25 $M_\odot$ and an inclination of 80°, although the profiles are not sensitive to the values chosen.

Figure 6 shows a simulation of the He II λ4686 line profile. The two-component simulation (wind and reimpact emission) bears comparison with the data in the general trends of the components. Much of the simulation (the treatment of broadening, the system parameters, the exact location of the reimpact emission, the relative intensities of wind and stream) is somewhat arbitrary, although reasonable changes do not alter the overall resemblance to the data. One problem, though, is that in order to obtain a good reproduction of the data I had to reduce the velocity of the reimpact emission by 25%. This is discussed further below.

4.2. Hβ

The Hβ line is broader than He II λ4686. Thus, it probably contains a component not present in He II λ4686. However, the likely candidate, disk emission, would give a double-peaked profile, of which there is little sign in the data. Therefore, I suggest that the Hβ line is composed largely of two components: a double-peaked disk profile with the center filled in by a single-peaked wind component similar to that in He II λ4686.

There is also a "disk reimpact" component, although it is weaker than that seen in PX And (HR94). It has a high velocity and, as in He II λ4686, it has maximum redshift at phase 0.9 and maximum blueshift at phase 0.4. In addition to these three emission components, there are at least two separate absorption features. One is the "phase 0.5

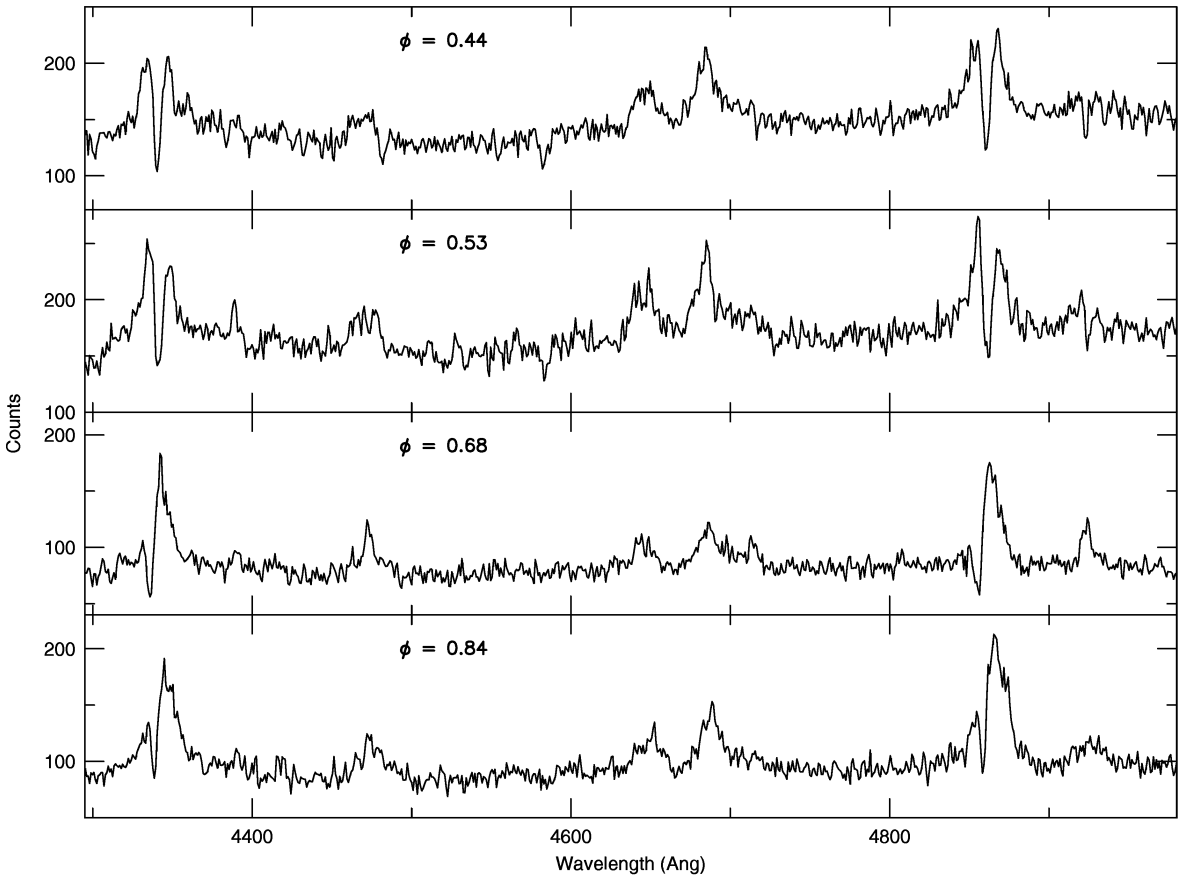

FIG. 7.—Sample 5 minute spectra illustrating the phase 0.5 absorption cores (*top two spectra*), and, later in the orbit, the blueshifted P Cygni absorption (*lower spectra*).

absorption" characteristic of SW Sex stars, a deep absorption feature in the line core near phase 0.5. The other is a weaker narrow trough to the blue of the line center, visible throughout the orbital cycle and showing a variation in velocity. Examples of the two absorption features in individual spectra are shown in Figure 7. The last feature in the data is an obvious increase in equivalent width during eclipse, implying that the line is eclipsed to a lesser degree than the continuum.

To attempt to reproduce the Hβ line, I started with the wind and reimpact components from the He II λ4686 line. To these, I added the profile of a Keplerian disk, using a radius 5×10^{10} cm. Now, if the stream emits along the length between its initial impact with the disk and its reimpact, it would produce lower velocity emission with a later phasing; in other words, the usual s-wave seen in many cataclysmic variables with maximum redshift near phase 0.2 and maximum blueshift near phase 0.7. There is no sign of such a feature in Hβ (nor indeed in the PX And data of HR94). If anything, the emission is depressed slightly along the track of this s-wave, although there is obvious absorption only around phase 0.5. Thus, to reproduce the data, the stream flowing over the disk would have to be a weak absorber, absorbing the light from the underlying disk, or at least not in emission. If some mechanism could increase the strength of the absorption near phase 0.5, the overflowing stream would explain the phase 0.5 absorption. Strong evidence that this is correct comes from Thorstensen et al.'s (1990) analysis of metal absorption lines in PX And, which, since they do not contain emission, give a reliable estimate of the absorption velocities. Their Figure 10 shows that the absorption is blueward of the emission centroid, is most visible between phases 0.2 and 0.6, and has a velocity variation first to the blue, then becoming redder. These velocity variations are exactly those of the track of the s-wave.

As an illustration, my Hβ model contains absorption from the stream between the initial impact and the reimpact. This is clearly too deep and narrow to explain the data at any phase except near 0.5, leaving two questions. First, does something reduce the absorption at other phases? As pointed out in HR94, one possibility is disk flaring. The rear of a flared disk will be more visible than the front, so obscuration of the disk by the stream would be more significant at phases $\sim$0.2–0.6, exactly when the absorption is seen in PX And (in my V1315 Aql data, there are so many other components that it is difficult to estimate the limits of the absorption). Another effect comes into play during eclipse. Not only will the stream itself be eclipsed at some phases, but so will the inner disk, which is expected to have Balmer absorption (e.g., Rutten et al. 1993), while the wind emission, being out of the plane, is eclipsed less. Thus, overall, absorption will be much reduced during eclipse, possibly contributing to the lack of a counterpart to the phase 0.5 absorption at these phases.

The second question is, can the stream produce the absorption anyway? In HR94 we estimated that the stream could produce absorption dips of 10% of the continuum (the maximum depth seen by Thorstensen et al. 1991) if the stream were $\frac{1}{3}r$ wide, where r is the disk radius. Disk flaring could reduce this by up to a factor 2 if the rear of the disk

were all that were visible. For comparison, the absorption in my model is set to 10% of the continuum and is clearly deeper than in my dataset. The model calculates velocities only, so it does not have an implicit spatial width; the velocity spread is set to 25% of the local stream velocity. Since it calculates only the velocities, rather than the spatial obscuration, it is not easy to introduce the effect of disk flaring in the current model, although clearly this should be done as the next stage in development. Finally, note that the intermediate polar FO Aqr shows a clear "absorption s-wave" that is visible throughout the orbital cycle (Hellier, Mason, & Cropper 1990).

4.2.1. *A P Cygni Trough?*

The other absorption feature seen in Hβ is a weak narrow trough consistently to the blue of the line center, visible through most of the orbital cycle and showing a variation in velocity compatible with the orbital motion of the white dwarf. Since I have already invoked the emission component of a wind, I suggest that this is an accompanying P Cygni trough. Although P Cygni troughs are not commonly seen in the optical spectra of nova-like variables (however common in the UV), they have been seen in at least one other system, BZ Cam (Patterson et al. 1996). In my model of Hβ, I have added a P Cygni trough with a blueshift of 170 km s^{-1} and the orbital velocity of the white dwarf.

The modeling by Hoare (1994) concludes that a wind contribution to the Balmer lines would be much weaker than to the He II lines, which argues against my interpretation. However, his model also predicts intensities that are too low in lines such as He II λ1640, which are clearly wind formed. Hoare suggests that increasing the wind loss rate, using a nonradial outflow, and allowing clumpy material would all increase the line emission.

4.2.2. *The Disk Reimpact Velocity*

As mentioned above, when computing the velocity of the reimpact emission I took the average of the stream and disk contributions and then reduced this velocity arbitrarily by 25%. The reason for this is that the reimpact feature in the He II λ4686 and Hβ line wings is only traceable to $\sim$1400 km s^{-1}, and this is reproduced by the 25% reduction. There are several possible ways of resolving the discrepancy. First, the stream could have lost energy in the initial impact with the disk, or in flowing over the disk, and so have a lower velocity than the free-fall velocity used in the model. Second, the reimpact emission could extend further into the line wings but not be traceable due to low S/N and contamination by other lines. The phase-averaged spectrum in Figure 1 shows that the Hβ line extends to $\pm$1600 km s^{-1}, which helps but still leaves an $\sim$15% discrepancy. Further, one could simply use a lower white dwarf mass. I have used 0.7 $M_\odot$, which is compatible with my measurement of the system parameters (§ 6) and near the mean mass of white dwarfs in cataclysmic variables. Reducing the mass to 0.4 $M_\odot$ gives the 25% velocity reduction but is uncomfortably low if the measurement of K_1 (§ 6) is reliable. Finally, it is possible that the free-fall trajectory of the stream could be distorted by interactions with the disk. If these deflected the stream further from the white dwarf, it would also reduce the velocities. Possibly, one or more of these reasons combine to resolve the discrepancy.

It is worth noting that in V795 Her, another star that might be explained by the disk overflow model, the high-velocity feature has a higher velocity relative to the rest of the line (Casares et al. 1996) and so does not have this problem. Similarly, in our modeling of PX And (HR94) we did not have to reduce the impact velocity to produce a good match to the data. It is unclear why V1315 Aql would behave differently, suggesting that a lower white dwarf mass is the most straightforward explanation.

4.2.3. *The Eclipse*

The last contribution to the model is the eclipse. The data show clearly that the lines are eclipsed less than the continuum. This is expected if the wind emission originates above the plane, and it could also arise if the central (optically thick) regions of the disk are eclipsed, leaving some outer parts (which are optically thin and therefore line emitting) uneclipsed. Unfortunately, we do not have sufficient information to include this in the model reliably: since the wind will vary on the scale of a few white dwarf radii, we would need to know the track of the eclipse to that accuracy. Therefore, I have increased the Hβ line intensity arbitrarily in my model to mimic the eclipse but made no further attempt to reproduce the data.

5. DOPPLER TOMOGRAMS

Doppler tomography is a useful alternative way of looking at spectra (see Marsh & Horne 1988). While phase-resolved spectra show how line-of-sight velocities change with orbital phase, a Doppler tomogram is an equivalent plot showing velocities relative to the rotating frame of the binary (typically, one plots velocity in the direction linking the stellar centers against velocity orthogonal to this line). I show tomograms of the data computed using the Fourier-filtered back projection technique. Essentially, a particle with a given velocity in the rotating frame will produce an s-wave in line-of-sight velocity (i.e., in phase-resolved spectra). A back projection simply sums the flux along each s-wave track in the data and plots it at the correct place in the tomogram. Taking a cross section of the tomogram through zero velocity at some angle gives back the line profile at the corresponding orbital phase.

A word of caution is in order: this technique assumes that all velocities are in the binary plane. It will not, therefore, handle features such as the P Cygni trough correctly. Further, it makes no allowance for changes in the intensity of features over an orbital cycle. Components that do vary, such as the phase 0.5 absorption, will again be handled incorrectly. Thus, tomograms need to be interpreted carefully.

Figures 8 and 9 show the tomograms of the He II λ4686 and Hβ lines. Figure 10 shows a schematic interpretation of the tomogram of a typical SW Sex star.

The wind emission has a roughly symmetric profile, varying with the orbital motion of the white dwarf. Therefore, it will appear as a bright spot at the location of the white dwarf in the tomogram. Since the He II λ4686 line consists mostly of this component, it dominates the tomogram. Surrounding the white dwarf in the Hβ tomogram is a ring of absorption, and beyond that is a circle of emission. The circle arises from the double-peaked profile of the disk emission. The absorption is formed from (1) the P Cygni trough: its blueshift causes it to be "defocused" in the tomogram, and therefore it appears as a ring rather than a spot, and (2) artifacts caused by the phase 0.5 absorption trough.

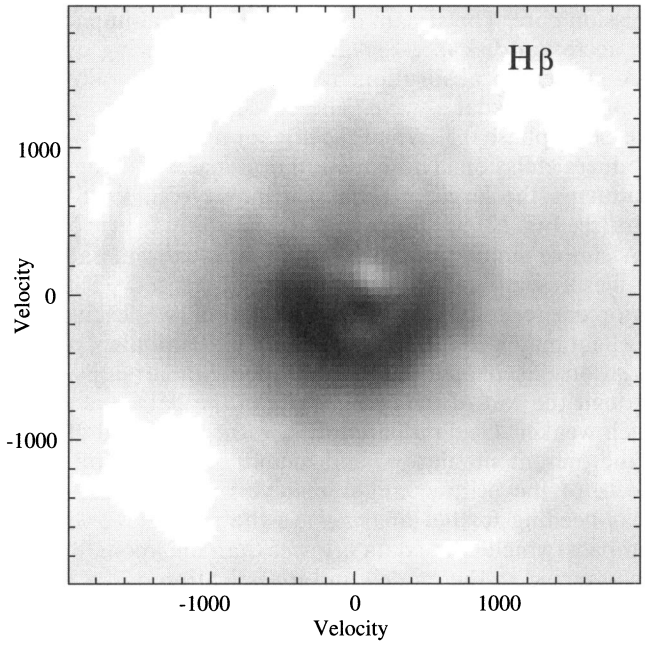

FIG. 8.—Tomogram of the Hβ line

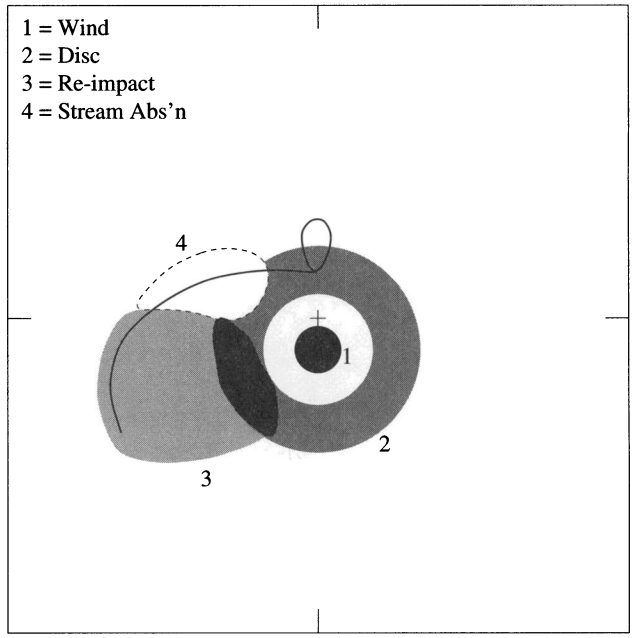

FIG. 10.—A schematic interpretation of the tomogram of an SW Sex star. The cross is the center of mass. The stream trails left from the Roche lobe of the secondary. The wind and disk produce emission centered on the white dwarf's velocity. The stream initially produces absorption, then emission that is heavily biased to lower velocities. The stream emission overlaps with the disk to produce a bright lower left quadrant.

The schematic tomogram shows the location of the secondary and the track of the mass transfer stream. Initially, the stream produces absorption; thus, the upper left quadrant of the tomogram is relatively faint (in contrast to the dwarf novae, in which emission from the stream/disk impact causes it to be bright).

Further along the trajectory, where it reimpacts the disk, the stream produces emission. This emission appears heavily biased to velocities lower than the free-fall trajectory, implying that kinetic energy has been lost through interaction with the disk. The Balmer tomograms are most intense where the emission from the reimpact overlaps with the disk component (lower left quadrant). This brightening should not be interpreted as a component in its own right. Our PX And data (HR94) showed the same effect and produced a very similar tomogram, the main difference being that PX And had little or no wind component. Conversely, the disk reimpact emission was stronger in PX And. Tomograms of PX And and V1315 Aql by Dhillon et al. (1991) and Still, Dhillon, & Jones (1995) are also consistent with this interpretation.

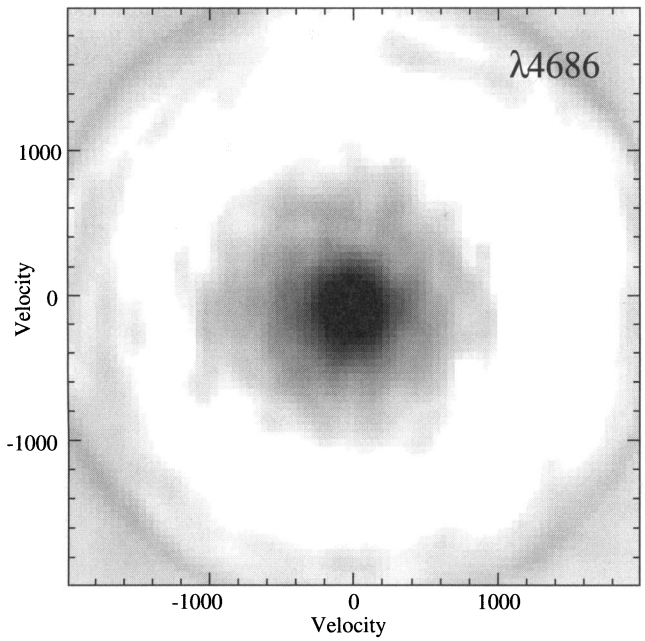

FIG. 9.—Tomogram of the He II λ4686 line. The outer ring is an artifact caused by the Bowen blend.

6. SYSTEM PARAMETERS

The line profiles in an SW Sex star are such a complex blend of components that the usual methods for deriving system parameters from CV spectra are useless. My attempts to decouple the components and obtain reliable velocities largely failed: the S/N is not sufficient for any multicomponent fitting program to cope with unless guided so heavily that the result is essentially achieved by eye. I did, though, obtain a semireliable estimate of the orbital velocity of the white dwarf. I assumed that the peak of the He II λ4686 line was due entirely to the wind (and that the reimpact emission is at a low level). Therefore, I fitted Gaussians to the line above half-height and recorded the central velocity (excluding profiles in eclipse). The velocities are plotted in Figure 11. A sinusoidal fit gives a red-to-blue crossing phase of 0.031 ± 0.015 (compared to 0.0 expected for the white dwarf). This discrepancy indicates that there is still some distortion due to the reimpact emission, though it is small. The amplitude was $K_1 = 112 \pm 8$ km s^{-1}, comparable with the $K_1 = 120 \pm 20$ reported by Dhillon et al. (1991), even though they took measurements biased towards the line wings, in which reimpact contamination would have been greater. Thus, my value of 112 km s^{-1} is probably close to the true white dwarf velocity.

From the constraints on eclipse width and inclination plotted by Dhillon et al. (1991), and using Patterson's (1984)

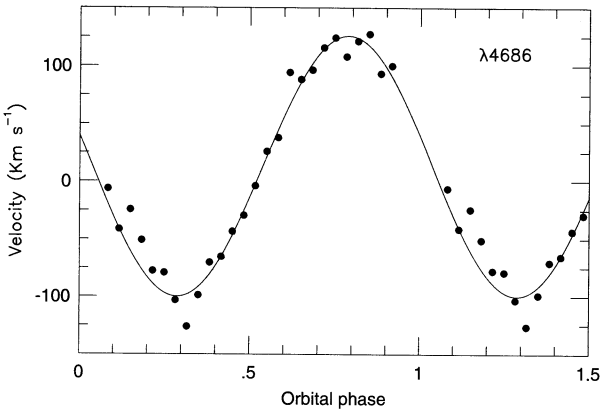

FIG. 11.—Velocities of the peak of He II λ4686

orbital period/secondary mass relation (which gives a secondary mass of 0.30 $M_\odot$), this value of K_1 propagates to a primary mass of 0.84 $M_\odot$ and an inclination of 83°. The uncertainty is dominated by the secondary mass: since secondaries often appear undermassive, I also illustrate a secondary mass of 0.25 $M_\odot$, which yields $M_1 = 0.61\ M_\odot$ and $i = 82°$.

I also attempted to measure the velocity variation of the P Cygni trough in the Hβ line. The measured values were not reliable due to the variations in the other components; however, the Hβ trough was consistently 170 ± 20 km s^{-1} blueward of the wind peak (as measured from He II λ4686).

7. SW SEX STARS

Previous attempts to model SW Sex stars have invoked either accretion disk winds (e.g., Dhillon et al. 1991) or disk overflow accretion (Hellier & Robinson 1994); neither could explain all features of the emission lines in SW Sex stars. This paper has attempted to combine both ideas and has shown that this can give a generally good account of the characteristic SW Sex spectral variations.

In this model, the single-peaked lines and non-Keplerian velocity profiles are largely caused by an accretion disk wind. The wind dominates He II λ4686, where it is seen entirely in emission. In the Balmer lines, it produces P Cygni profiles, with an absorption trough blueward of the emission core. The stream overflows the initial impact with the accretion disk (see Fig. 12) and while flowing over the disk is seen in absorption, removing emission along the track of the usual s-wave. The absorption becomes more intense at phase 0.5. When the stream reimpacts the disk it produces emission. This emission dominates the line wings, producing the large phase distortions typical of SW Sex stars (see Fig. 12).[1]

A simple simulation based on these ideas generates line profiles resembling the data in most respects. The only major discrepancy is that the simulation, while giving an excellent match to the absorption features and their velocity variations at phases 0.2–0.6, predicts similar absorption through the rest of the cycle, while in the data it is at best much weaker. Using a flared disk, rather than the flat disk of the present simulation, and further consideration of the effects of the eclipse, might resolve this problem. Other areas needing further analysis are the velocity of the disk reimpact (which in the data is lower than the free-fall velocities assumed in the model) and investigation of the optical line emission from a wind. In addition, quality data of an SW Sex star through eclipse is needed to test the model; my current data do not have sufficient time resolution or S/N for this.

If this model is correct, an SW Sex star seems to be a cataclysmic variable with a strong accretion disk wind and a stream overflowing the accretion disk. A high mass transfer rate might explain both these phenomena. It is generally accepted that wind intensity correlates with the rate of accretion onto the white dwarf (for instance, dwarf novae show winds in outburst but not in quiescence). It is less clear, though, whether disk overflow is affected by mass transfer rate, but the evidence is consistent with this. For instance, disk overflow is seen mostly in nova-like variables and not in the lower $\dot{M}$ dwarf novae. EX Hya is one dwarf nova that has shown disk overflow accretion, but only during an outburst that Hellier et al. (1989) suggested was caused by a burst of mass transfer (although this interpretation is

[1] In HR94, we suggested that the s-wave from the reimpact causes the single-peaked profiles by filling in the disk double peaks at some phases; while this is true to some extent, it is not a sufficient explanation and cannot account for lines such as He II λ4686, in which the re-impact emission is weak; for this, a wind is required.

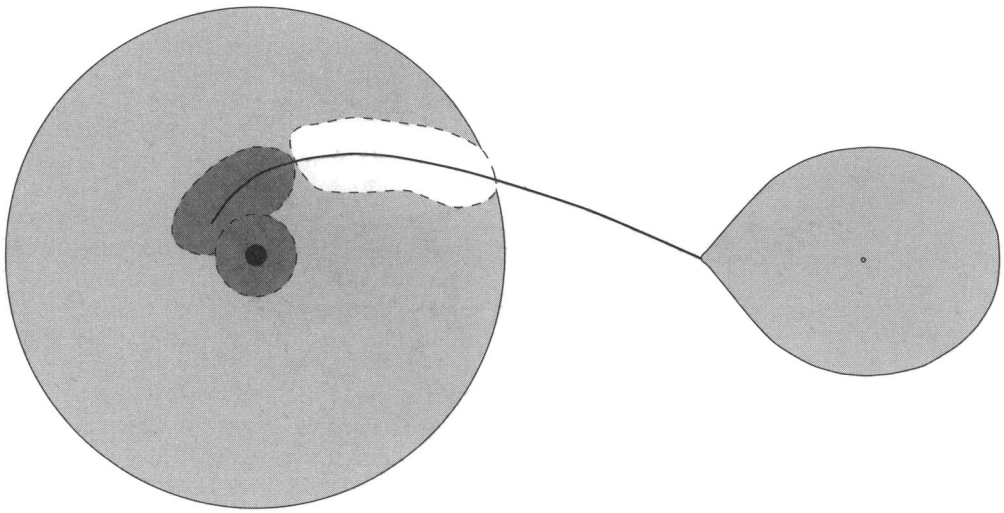

FIG. 12.—A schematic illustration of our model for an SW Sex star, showing disk overflow causing absorption and then emission. An accretion disk wind from near the white dwarf adds to the emission, filling in the double-peaked profile produced by the accretion disk.

controversial). Strong evidence for disk overflow is also seen in intermediate polars (e.g., FO Aqr; Hellier 1993), which are also high $\dot{M}$ systems.

The characteristics of SW Sex stars do seem sufficiently distinctive to deserve a label. Leaving "SW Sex star" defined by observational characteristics (as done by Thorstensen et al. 1991) fulfills this function and is not vulnerable to revision. However, if we are confident that disk overflow accretion is the cause of the peculiarities of SW Sex stars, we could define the term by its presence (e.g., HR94).

In this paper, though, we have seen that a strong wind plays a role also, and that both phenomena might be related to a high $\dot{M}$. A recent synthesis of observational and theoretical results (e.g., Osaki 1996) has led to the idea that a range of mass transfer rates in CVs below the period gap leads to a sequence of outburst properties: from WZ Sge stars (low $\dot{M}$), to SU UMas, to ER UMa stars, to permanent superhumpers (high $\dot{M}$). Above the period gap there is a transition from U Gem stars (low $\dot{M}$), to Z Cam stars, to nova-like variables (high $\dot{M}$). In this spirit, SW Sex stars can be regarded as extreme high mass transfer rate nova like variables, with the high $\dot{M}$ resulting in disk overflow and a strong wind. The other two characteristics noted by Thorstensen et al. (1991) are then explained as follows: SW Sex stars tend to be eclipsing, since the characteristic distorted emission lines are detected more easily in these systems. Further, SW Sex stars tend to have orbital periods of 3–4 hr since CVs in this range have higher $\dot{M}$ values. This is probably because such systems have the smallest separations amongst the high-$\dot{M}$ systems above the period gap, and so irradiation of the secondary will be most significant. Warner (1995) suggests that these systems can exist in two states, with periods of anomalously high $\dot{M}$ enhanced by irradiation, compensated for by episodes of very low $\dot{M}$. We can identify the high states with SW Sex behavior and note that some of these stars (BH Lyn, DW UMa) show VY Scl low states.

To secure this hypothesis, we need a better understanding of disk overflow accretion, particularly whether it is caused by high $\dot{M}$ or by something else. While theorists address this question, observers should investigate its incidence in all types of cataclysmic variables.

I thank Cyndi Froning for her valuable assistance at the McDonald 2.1 m telescope. The data were obtained while I was a Hubble Fellow at the University of Texas at Austin.

REFERENCES

Annis, J. T. 1986, Inf. Bull. Variable Stars, 2858
Casares, J., Martínez-Pais, I. G., Marsh, T. R., Charles, P. A., & Lazaro, C. 1996, MNRAS, 278, 219
Dhillon, V. S., Marsh, T. R., & Jones, D. H. P. 1991, MNRAS, 252, 342
Hellier, C. 1993, MNRAS, 265, L35
Hellier, C., Mason, K. O., & Cropper, M. 1990, MNRAS, 242, 250
Hellier, C., Mason, K. O., Smale, A. P., Corbet, R. H. D., O'Donoghue, D., Barrett, P. E., & Warner, B. 1989, MNRAS, 238, 1107
Hellier, C., & Robinson, E. L. 1994, ApJ, 431, L107 (HR94)
Hoare, M. G. 1994, MNRAS, 267, 153
Honeycutt, R. K., Schlegel, E. M., & Kaitchuck, R. H. 1986, ApJ, 302, 388
Lubow, S. H. 1989, ApJ, 340, 1064
Marsh, T. R., & Horne, K. 1988, MNRAS, 235, 269
Osaki, Y. 1996, PASP, 108, 39
Patterson, J. 1984, ApJS, 54, 443
Patterson, J., Patino, R., Skillman, D. R., Harvey, D., Thorstensen, J. R., & Ringwald, F. A. 1996, AJ, 111, 2422
Rutten, R. G. M., Dhillon, V. S., Horne, K., Kuulkers, E., & van Paradijs, J. 1993, Nature, 362, 518
Shafter, A. W., Hessman, F. V., & Zhang, E. H. 1988, ApJ, 327, 248
Still, M. D., Dhillon, V. S., & Jones, D. H. P. 1995, MNRAS, 273, 863
Thorstensen, J. R., Ringwald, F. A., Wade, R. A., Schmidt, G. D., & Norsworthy, J. E. 1991, AJ, 102, 272
Warner, B. 1995, Cataclysmic Variable Stars (Cambridge: Cambridge Univ. Press)